J Wood Sci (2006)
DOI 10.1007/s10086-005-0747-2

ORIGINAL ARTICLE

Akio Koizumi · Takuro Hirai

Evaluation of the section modulus for tree-stem cross sections of irregular shape

Received: April 25, 2005 / Accepted: June 22, 2005

Abstract The effect of section modulus, as estimated for tree stems of irregular cross section with hollow trunks, on windthrow resistance is discussed. The sample trees were 12 aged poplar trees growing along the roadside in Sapporo. Binarized bitmap images of photographs of the crosscut surface of the sample tree stems were used to calculate numerical solutions for section moduli. The error for image resolution was simulated to less than 1% under the condition in which the image was divided into more than 400 pixels. The coefficient of variation in section modulus concerning six neutral axis directions in a horizontal plane was 11%–14%. The reduction in section modulus caused by decay or hollow trunk was 36%–56% of the full cross section. The effect of section modulus on critical wind velocity was found to be considerable. The critical wind velocity calculated for some of the sample trees was less than 40 m/s, and these trees were considered to be in danger of bending failure of the stems.

Key words Windthrow resistance · Section modulus · Bitmap image · Hollow trunk · Bending strength

Introduction

Aged trees of large size with decayed hollow cross sections are in danger of windthrow by gales and those growing along the roadside or in parks have the potential to cause property damage or personal injury. Therefore, reinforcement or felling of such trees is required. Recently, environmental protection concerns have resulted in a tendency for large trees to be maintained or preserved rather than felled. Therefore, the establishment of a method of quantitative evaluation for tree resistance to wind force is desirable.

The moment that causes windthrow is induced by the wind force applied on the tree crown and bole. Wind tunnel studies have been undertaken to obtain drag coefficients for various tree species.[1–6] Mayhead[4] analyzed test data from full-scale experiments performed at a wind tunnel of the Royal Aircraft Establishment at Farnborough, UK, in the 1960s. The results indicated a reduction in drag coefficient with increased wind velocity because the projected frontal area of the tree crown decreased with wind velocity. It was concluded that the drag coefficients converged to nearly constant values at the range of wind velocity likely to cause windthrow. The drag coefficients at 30 m/s were determined as 0.41 for tree species having a dense crown (grand fir and Sitka spruce), which receive a large wind pressure per projected area, and 0.31 for pines (Corsican pine, lodgepole pine, and Scots pine).

Koizumi[7] discussed the failure mode and critical wind velocity for plantation-grown coniferous species of 19- to 45-year-old trees. The possible failure modes were classified into bending failure of tree stem and uprooting. The critical height at which bending failure occurs was estimated to be approximately 20% of the tree height for plantation-grown conifers.[7] In contrast, aged trees having decayed or hollow trunks (examined in the present study) were estimated to fail at the stem, near ground level, because of the decrease in effective cross section that is necessary to withstand the bending moment. Although Mattheck[8] indicated that the thin wall of the hollow tree trunk would fail by flattening of the cross section or by shell buckling, quantitative evaluation of the critical moment that causes flattening or shell buckling is difficult because the vertical expansion of the hollow in a trunk, as well as the horizontal distribution, must be known.

The section modulus of an irregularly shaped cross section, which determines the critical bending moment, could not be solved analytically. The goal of the present study was to discuss the method by which to evaluate the section modulus for trees having irregularly shaped or hollow cross

A. Koizumi (✉) · T. Hirai
Graduate School of Agriculture, Hokkaido University, N9 W9, Kita-ku, Sapporo 060-8589, Japan
Tel. +81-11-706-3340; Fax +81-11-706-3636
e-mail: akoizumi@for.agr.hokudai.ac.jp

sections using bitmap images of photographs of the cross section of the tree stems. The critical wind velocity that causes bending failure was also estimated for the sample trees.

Materials and methods

Sample trees

The sample trees were 12 black poplars (*Populus nigra* var. *italica*) that were growing along a street running north to south on the campus of Hokkaido University, Sapporo (Fig. 1). The trees were planted in the 1930s and the ages of these trees were estimated to be approximately 60–70 years. Accurate ages could not be determined because the heartwood near the pith was lost due to decay. The trees were felled due to the potential for collapse based on a safety diagnosis by a tree doctor. The diagnosis report included measurements of the tree height, crown length, crown width, diameter at breast height, and diameter and thickness of sound wood without bark at the critical height near ground level (Table 1). The thickness of sound wood listed in Table 1 was measured by a tree doctor using a resistograph.[9]

Fig. 1. Sample poplar trees planted in a row (before felling)

Evaluation of effective cross section

A butt log was collected from each tree after felling and the crosscut surface at a height of 1 m above ground level was photographed with a digital camera for evaluation of effective cross section. A 1-m-long bar lying across the crosscut surface was used as a scale pointing in the north and south directions (Fig. 2a). In order to determine the thickness of sound wood without decay, the penetrating depth parallel to the grain was measured using a Pilodyn tester every 20 mm from the bark side in eight radial directions on the crosscut surface, as shown in Fig. 2a. In order to examine the relationship between penetration depth and the extent of decay, 36 small specimens ($20 \times 20 \times 60$ mm) were cut from the adjacent section of Pilodyn-tested points of sample logs and were tested for compressive strength parallel to the grain in green condition. After the test, the specimens were dried at 20°C and 60% relative humidity (RH) and were measured with respect to wood density. In addition, 6 small clear specimens ($20 \times 20 \times 300$ mm) were cut from upper logs of the sample trees and were tested in green condition for bending strength to estimate the critical wind velocity that causes breakage due to wind.

Evaluation of section modulus

Bitmap images of the photographs for the cross section were binarized into black and white images in which white areas represented wood (with or without decay) (Fig. 2b,c). The section modulus for the wood area was calculated based on the white areas of the binarized images as follows:

Table 1. Dimensions of sample poplar trees

No.	H (m)	CL (m)	CW (m)	DBH (cm)	H_c (m)	D_c (cm)	T_c (cm)
1	27	23.9	7.7	123	1.5	97.0	16.5
2	21	18.6	5.4	95	0.6	80.5	8.0
3	28	23.0	9.1	97	0.9	85.0	19.0
4	30	26.3	7.8	82	1.0	76.5	11.0
5	30	25.0	8.5	91	1.0	78.0	12.5
6	30	25.2	8.9	100	1.5	90.0	10.0
7	30	25.2	8.3	97	1.1	83.0	9.5
8	30	24.5	9.4	107	1.1	98.5	9.0
9	29	24.5	8.8	106	1.1	86.5	12.0
10	28	24.5	7.4	90	1.5	75.0	8.5
11	28	24.0	8.0	85	1.4	82.5	8.0
12	29	24.6	8.9	105	1.1	94.5	20.0

H, tree height; CL, crown length; CW, crown width; DBH, breast height diameter; H_c, surveyed height considered to be critical concerning windbreak by a tree doctor; D_c, average diameter at surveyed height; T_c, average sound wood thickness at surveyed height

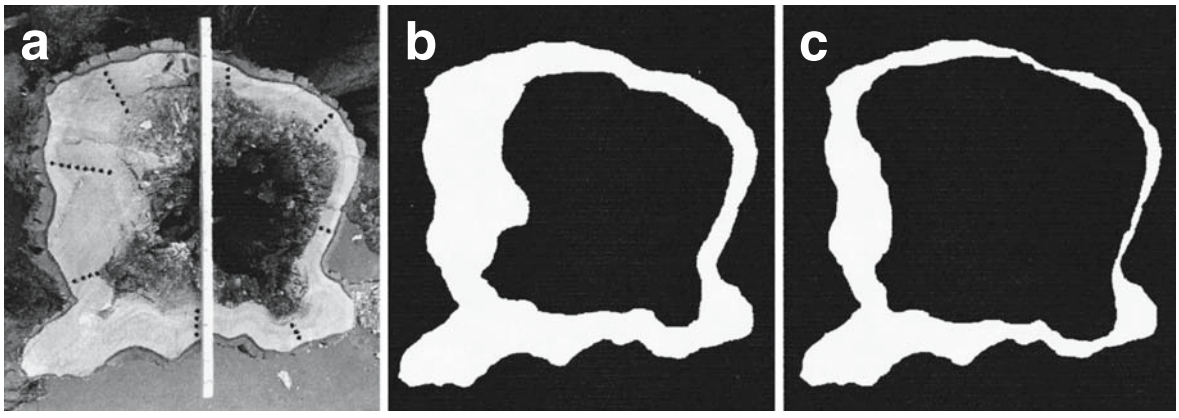

Fig. 2a–c. Example of photograph and binarized images of a cross section (tree no. 5). **a** Photograph of a cross section. *Black dots* indicate Pilodyn-tested points. *White bar*, 1 m. **b** Binarized image of the photograph for wood area (image A). **c** Binarized image of the photograph for sound wood area estimated by Pilodyn tests (image B)

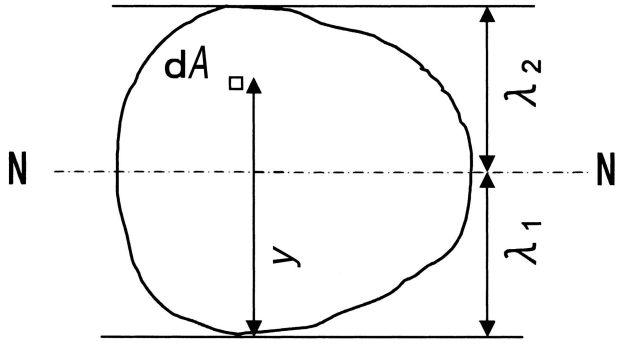

Fig. 3. Dimensions of irregularly shaped cross section

At first, the position of the neutral axis was determined by dividing the geometrical moment of the area by the area of the wood, according to the following equation, by scanning the images:

$$\lambda_1 = \frac{\sum y\mathrm{d}A}{\sum \mathrm{d}A} \tag{1}$$

where λ_1 is the distance between a horizontal line passing through the lower edge of the wood area and the neutral axis, y is the distance between the horizontal line and a finite small area (dA) which was taken as a pixel among the white area in the binarized image (see Fig. 3).

To calculate for the cross section on which Young's modulus of the wood is not uniform, ydA and dA in Eq. 1 should be weighted with Young's modulus. In the present study, Young's modulus of the wood was assumed to be uniform over the wood area because it was difficult to weight with variable Young's modulus using a binarized image.

Then, the moment of inertia (I) and the section modulus (Z) were calculated by numerical analysis following Eqs. 2 and 3:

$$I = \sum \left(y - \lambda_1\right)^2 \mathrm{d}A \tag{2}$$

$$Z = \frac{I}{\max\left(\lambda_1, \lambda_2\right)} \tag{3}$$

Estimation of critical wind velocity

Critical wind velocity was estimated based on the simplification of assumptions as follows:

1. Uniform wind pressure acts on the projected crown area (A) calculated as a product of the crown width and crown length.
2. The height of the wind pressure center (H_w) is half of the crown length.
3. Trees are assumed to fail in bending at a height of 1 m above ground level without uprooting.
4. The effects of neighboring trees on wind velocity are neglected.
5. The wind pressure acting on the stem below the crown is neglected.

Trees were analyzed as vertical cantilever beams fixed at ground level. Drag coefficients (C_D) for the poplar crown were calculated from Eq. 4, as determined from the empirical equation for the data for the Scotch pine reported by Mayhead.[4]

$$C_D = \frac{3.22}{v} + 0.186 \tag{4}$$

where v is the wind velocity (m/s).

The critical bending moment at a height of 1 m above ground level (M_c) is expressed as follows:

$$M_c = \frac{1}{2} C_D \rho v_c^2 A\left(H_w - 1\right) = Z\sigma_b \tag{5}$$

where ρ is the air density (1.20 kg/m^3), v_c is the critical wind velocity, and σ_b is the bending strength of the wood.

Finally, the critical wind velocity (v_c) was calculated using the following equation, which was obtained by rearranging Eqs. 4 and 5:

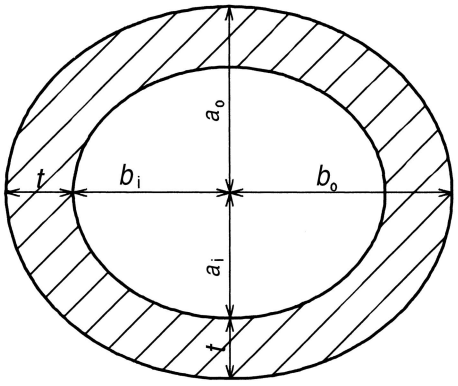

Fig. 4. Sample cross section of elliptical cylinder used for calculation of errors in numerical solution. $b_o = 1.2a_o$; $t/b_o = 0.3$

$$\nu_c = \frac{-3.22 + \sqrt{10.4 - 0.744C}}{0.372} \tag{6}$$

where

$$C = -\frac{2Z\sigma_b}{1.2A(H_w - 1)}$$

Results and discussion

Errors in numerical solution due to image resolution

The cross section of an elliptical cylinder (shown in Fig. 4) was considered to discuss the error that arose in numerical solution compared with the analytical solution in relation to the image resolution. The analytical solutions for the moment of inertia (I) and the section modulus (Z) of the elliptical cylinder were calculated according to the following equations.

$$I = \frac{\pi}{4}\left(a_o^3 b_o - a_i^3 b_i\right) \tag{7}$$

$$Z = \frac{I}{a_o} \tag{8}$$

where the a and b dimensions are defined in Fig. 4. Numerical solutions for the ellipse image were calculated for 20%, 40%, 60%, 80%, and 100% resolution of the original image, which spans 620 pixels in the direction of the major axis (Fig. 5). The ratios of the numerical solution to the analytical solution were less than 1.01 under the condition that the long diameter ($2b_o$) was divided into more than approximately 400 pixels for the images. Although the cross-sectional shapes of the sample trees were complicated with uneven circumferences, which introduces more errors in the numerical solution compared with the case of a simple elliptical cylinder, the errors due to the image resolution were considered to be negligible because the resolution of the photograph for the sample trees exceeded 600 pixels in diameter.

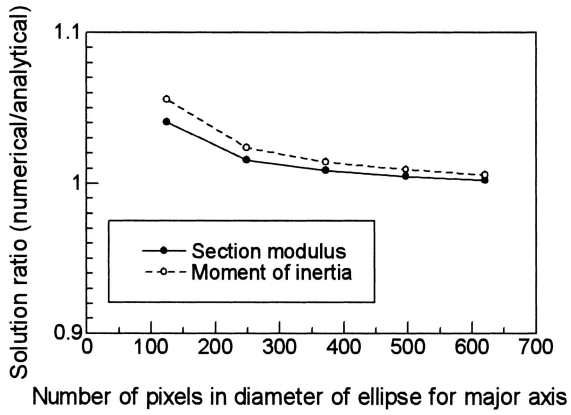

Fig. 5. Errors in numerical solution in relation to resolution of the elliptical cylinder image shown in Fig. 4

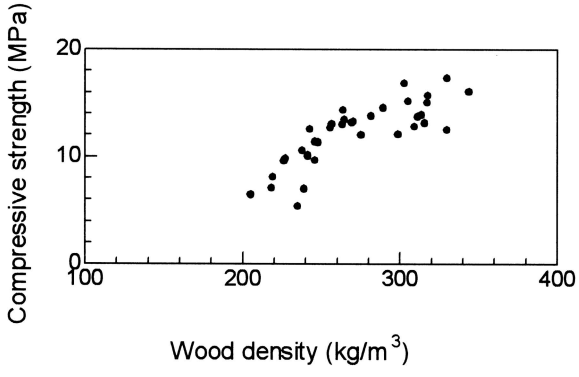

Fig. 6. Relationship between wood density and compressive strength parallel to the grain for small specimens cut from the sample logs including decaying wood

Effective cross section

As shown in Fig. 6, the relationship between wood density (moisture content 11%) and compressive strength parallel to the grain of the small specimens in green condition changed at a wood density of approximately 240 kg/m^3 and a compressive strength of 10 MPa. The compressive strength for the parts of specimens that had wood densities of less than 240 kg/m^3 showed lower values than predicted by linear regression, and these parts were considered to contain decaying wood. This result was consistent with published data[10] for the specific gravity and compressive strength of balsam poplar (*Populus balsamifera*), which are 0.31 and 11.6 MPa, respectively. The penetration depth obtained using the Pilodyn tester is a good indicator of wood density.[11] Negative correlation between Pilodyn penetration and wood density for the small specimens was observed, as shown in Fig. 7. The boundary value between sound wood and decaying wood was taken to be 33 mm in Pilodyn penetration, which corresponds to a wood density of 240 kg/m^3, according to the regression line shown in Fig. 7.

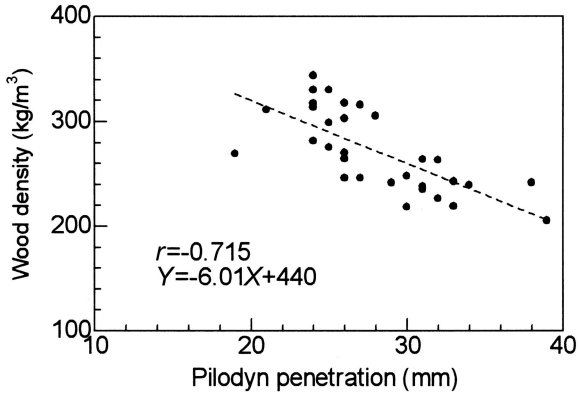

Fig. 7. Relationship between Pilodyn penetration and wood density for small specimens

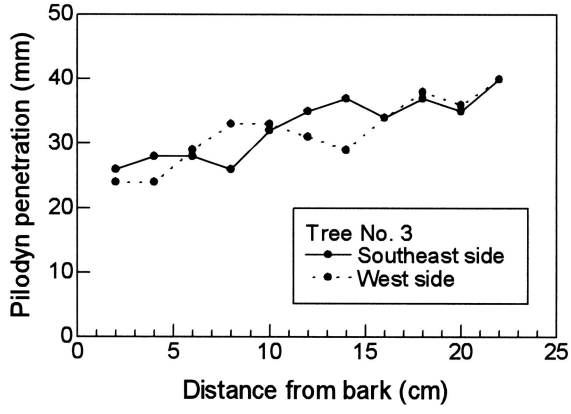

Fig. 8. An example of Pilodyn penetration trend observed in radial directions on the crosscut surface

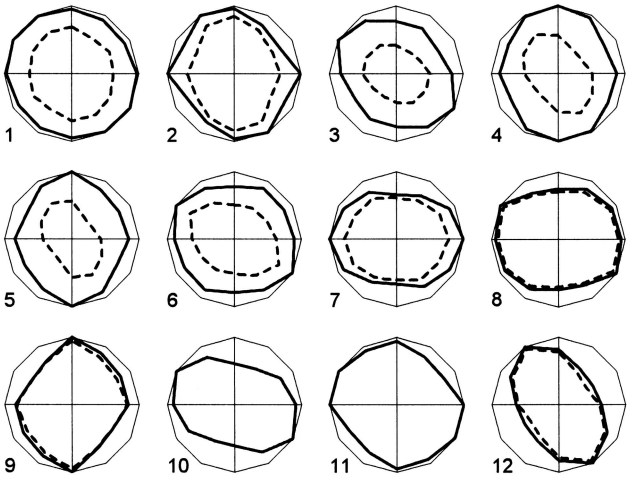

Fig. 9. Section modulus ratio concerning six moment directions for all sample trees. Twelve trees were numbered sequentially from south to north in the planted row. Upward direction indicates north. *Solid line*, calculation based on image A; *broken line*, calculation based on image B. Both images coincided for nos. 10 and 11

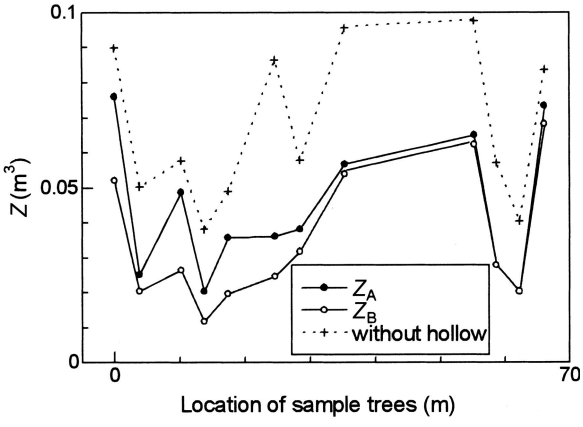

Fig. 10. Calculated section moduli of sample trees in relation to their location shown as the distance from the south end tree (tree no. 1). $Z_{A,B}$, section moduli numerically calculated for images A and B

The penetration depth obtained using the Pilodyn tester was greater on the inner side of the cross section than on the outer side (Fig. 8). According to the above definition, the distances from the outside surface to the boundary between the sound wood and the decaying wood were 8 cm on the west side and 10 cm on the southeast side. As an example, approximate boundaries determined for the sample tree (no. 5) are shown in Fig. 2, in which image A shows the visually determined wood area and image B shows the wood area determined by the Pilodyn penetration method. The section modulus is considered to be in the range of the upper bound of image A and the lower bound of image B.

Variation in section modulus concerning moment direction

The windbreak resistance varies with the load direction because the section modulus is not constant for unevenly shaped cross sections concerning the neutral axis direction. Six section moduli (Z) were calculated for the directions designated by 30-degree intervals in the horizontal plane of the sample trees, as shown in Fig. 9, where each section modulus is shown as a ratio to the maximum section modulus of the tree. Values related to solid line (Z_A) and broken line (Z_B) were calculated based on images A and B, respectively, in Fig. 2. Although the sample trees were planted in a row running north to south, no correlation between the moment resistance and orientation of the stem was found. The coefficients of variation for the ratio were 11.4% and 14.2% for Z_A and Z_B, respectively. The average section modulus for the six directions is discussed in the following section.

Effects of the hollow cross section on section modulus

The section modulus decreases to some extent as decay develops in the heartwood region. The calculated section moduli for the sample trees are shown in Fig. 10 in relation

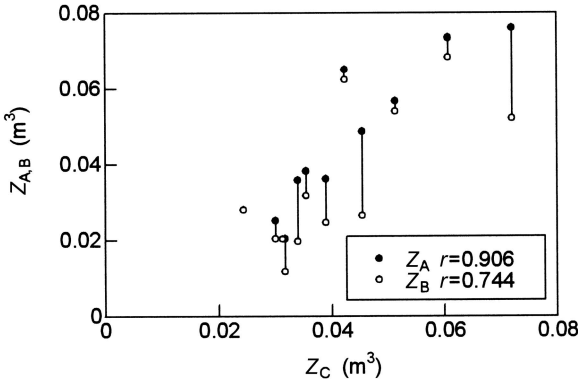

Fig. 11. Comparisons of section moduli. $Z_{A,B}$, section moduli numerically calculated for images A and B; Z_C, calculated for cylindrical cross section based on the average diameter and sound wood thickness measured by a tree doctor with a resistograph; r, coefficients of correlation between Z_C and $Z_{A,B}$

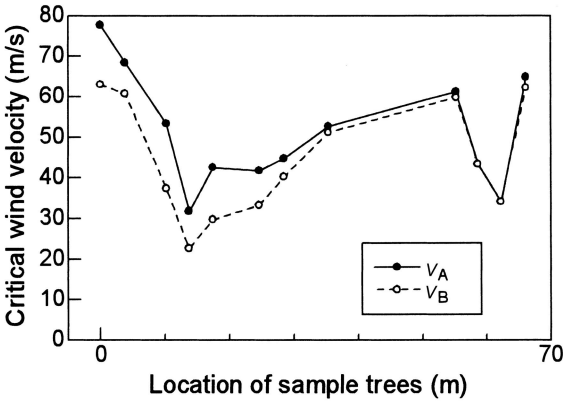

Fig. 12. Critical wind velocity estimated for the sample trees in relation to their location shown as the distance from the south end tree (tree no. 1). v_A, calculated for image A; v_B, calculated for image B

to their location in the planted row. The section moduli for the trees located at the end of the row were found to be large as a result of vigorous growth in open space. The average decreases in section modulus caused by the hollow cross section were 36% and 50% for images A and B, respectively.

The section modulus based on the cylindrical cross section (Z_C) was calculated from Eq. 9 using the diameter and sound wood thickness of sample trees measured by a tree doctor in advance of felling (see Table 1):

$$Z_C = \frac{\pi\left(r_o^4 - r_i^4\right)}{4r_o} \tag{9}$$

where r_o is the average radius of the trunk without bark and r_i is the average radius of the hollow space.

Adequate correlation was found for the section modulus between the calculation based on the cylindrical assumption and that based on image A (Fig. 11). Average section modulus ratios were 1.024 and 0.824 for Z_A/Z_C and Z_B/Z_C, respectively. Therefore, rough estimation of section modulus can be performed using the cylindrical-shape assumption. However, accurate estimation for individual trees and/or load directions should be based on numerical solutions that consider irregular shape.

Critical wind velocity

Wind velocities that cause bending failure for the sample trees were estimated by Eq. 6. The bending strength (σ_b) for a poplar tree was assumed to be 27.7 MPa, which was derived as the lower limit (fifth percentile) of the bending strength measured for the small clear specimens in the green condition. Effects of defects such as knots on bending properties for trees or logs were considered to be small, because wood fibers at the sapwood surface are not cut by lumber sawing.[12]

The tendency of critical wind velocity in relation to tree location (Fig. 12) was similar to that of section modulus shown in Fig. 10. The effect of section modulus on critical wind velocity was found to be considerable. The critical wind velocities calculated for 5 of 12 sample trees for image B were less than 40 m/s, and these trees were considered to be in danger of windthrow because the maximum wind velocity adopted for the building design code for the Sapporo area is 32 m/s.

Conclusions

The method of evaluating section modulus and its effects on windthrow resistance for poplar trees having irregularly shaped cross sections were discussed and the following conclusions were obtained:

1. The section modulus of trees having an irregularly shaped and hollow cross section could be calculated with numerical analysis based on an image of the sound wood area. The error involved with image resolution was simulated to less than 1% when the image was divided into more than 400 pixels.
2. The coefficient of variation in section modulus concerning six neutral axis directions was 11%–14%.
3. The reduction in section modulus caused by decayed or hollow trunks was 36%–56% of the full cross section.
4. Rough estimation of the average section modulus is possible based on the assumption of a cylindrical section. However, accurate estimation for individual trees and/or load directions requires a numerical solution considering irregular shape.
5. The effect of the section modulus on the critical wind velocity was found to be considerable. The critical wind velocity calculated for some of the sample trees was less than 40 m/s and these trees were considered to be in danger of windthrow based on the assumptions used in this study.

The failure modes of uprooting or shell buckling for thin-walled cylinders were not considered in the present study.

The calculation for critical wind velocity was done based on average section modulus for six directions instead of minimum section modulus. Therefore, the critical wind velocity evaluated herein may be too large and overestimated.

Photographs of crosscut surfaces of sample trees were used for the analysis in the present study. Nondestructive evaluation of effective cross section will be required for the purpose of safety diagnosis for trees in parks or along the roadside.

Acknowledgment The authors thank Ms. Akiko Miura for her kind assistance in the experimental work.

References

1. Hirata T (1953) Fundamental studies on the formation of cutting series (2) (in Japanese). Bull Tokyo Univ Forest 45:67–88
2. Fraser AI (1964) Wind tunnel and other related studies on coniferous trees and tree crops. Scot Forest 18:84–92
3. Leiser AT, Kemper JD (1973) Analysis of stress distribution in the sapling tree trunk. J Am Soc Hortic Sci 98:164–170
4. Mayhead GJ (1973) Some drag coefficients for British forest trees derived from wind tunnel studies. Agr Meteorol 12:123–130
5. Johnson RC, Ramey GE, O'Hagan DS (1982) Wind induced forces on trees. J Fluid Eng 104:25–30
6. Murakami S, Deguchi K, Takahashi T (1984) Shelter effects of trees as wind-breaks (in Japanese). Proceedings of Symposium on Wind Engineering, Tokyo, pp 129–136
7. Koizumi A (1987) Studies on the estimation of the mechanical properties of standing trees by non-destructive bending test (in Japanese). Res Bull Coll Exp Forest Hokkaido Univ 44:1329–1415
8. Mattheck C (1998) Design in nature. Springer, Berlin, Heidelberg, New York, pp 1–276
9. Rinn F, Schweingruber F-H, Schär E (1996) RESISTOGRAPH and X-ray density charts of wood comparative evaluation of drill resistance profiles and X-ray density charts of different wood species. Holzforschung 50:303–311
10. Forest Products Laboratory (1987) Wood handbook. USDA Forest Service, Madison, pp 4.1–4.45
11. Cown DJ (1978) Comparison of the Pilodyn and Torsiometer methods for the rapid assessment of wood density in living trees. New Zeal J For Sci 8:384–391
12. Koizumi A, Ueda K (1987) Bending and torsional properties of logs (in Japanese). Res Bull Coll Exp Forest Hokkaido Univ 44: 355–380